



Proceeding Paper

Assimilation of In Situ Meteorological Data to Optimize a Weather Service for Mosquito Control [†]

Stergios Kartsios ^{1,*}, Eleni Katragkou ¹, Maria-Chara Karypidou ¹, Sandra Gewehr ² and Spiros Mourelatos ²

¹ Department of Meteorology and Climatology, School of Geology, Faculty of Sciences, Aristotle University of Thessaloniki, 54124 Thessaloniki, Greece; katragou@auth.gr (E.K.); karypidou@geo.auth.gr (M.-C.K.)

² Ecodevelopment S.A., Filyro P.O. Box 2420, 57010 Thessaloniki, Greece; gewehr@ecodev.gr (S.G.); smourelat@gmail.com (S.M.)

* Correspondence: kartsios@geo.auth.gr

† Presented at the 16th International Conference on Meteorology, Climatology and Atmospheric Physics—COMECPA 2023, Athens, Greece, 25–29 September 2023.

Abstract: This study investigates the impact of data assimilation to the weather forecasts produced within the project “MOSQUITO VISION”, concerning the development of a digital application for mosquito nuisance prediction. The in situ meteorological data used for the assimilation are retrieved from the Region of Central Macedonia (RCM) climate data hub, currently including 49 meteorological stations compliant with WMO requirements. Here, we assess the numerical system’s performance by ingesting available observations over the RCM through two different data assimilation techniques using the Weather Research and Forecasting model. The results indicate that there is no significant added value to the assimilated weather forecasted fields over the area of interest (RCM), and the assimilated signal is diminishing relative quickly due to non-linear processes. This study is funded under the Greek Research and Innovation Strategies for Smart Specialization call (RIS 3, project code: KMP6_077890).

Keywords: data assimilation; numerical weather prediction; WRF; mosquito; West Nile virus



Citation: Kartsios, S.; Katragkou, E.; Karypidou, M.-C.; Gewehr, S.; Mourelatos, S. Assimilation of In Situ Meteorological Data to Optimize a Weather Service for Mosquito Control. *Environ. Sci. Proc.* **2023**, *26*, 5. <https://doi.org/10.3390/environsciproc2023026005>

Academic Editors: Konstantinos Moustiris and Panagiotis Nastos

Published: 23 August 2023



Copyright: © 2023 by the authors. Licensee MDPI, Basel, Switzerland. This article is an open access article distributed under the terms and conditions of the Creative Commons Attribution (CC BY) license (<https://creativecommons.org/licenses/by/4.0/>).

1. Introduction

Mosquito-borne diseases pose an unprecedented threat to public health, since mosquitoes are considered to cause the largest number of deaths in humans. Malaria, Dengue and Yellow Fever, Zika Virus Disease and West Nile Virus are some of the most common mosquito-borne diseases. Since the late 1990s, there has been a considerable increase in the number of invasive mosquitoes in Europe. Greece, Italy, France and Germany serve as excellent examples in terms of implemented projects aiming to enact control and response actions against mosquito-borne diseases by their national authorities.

Mosquitoes of the genus *Culex* are responsible for transmitting the West Nile virus. In Greece, they are abundant and common, while the first major outbreak occurred in 2010 in the Region of Central Macedonia (RCM) [1]. Since then, West Nile virus has acquired an endemic status over the region, with 599 cases of West Nile neuroinvasive disease reported by the National Public Health Organization (2010–2022). In 2022, Greece was the second most seriously affected European country with 284 reported human cases of WNV, following Italy (586 cases) [2,3].

West Nile virus is a weather-sensitive disease since the vector through which it is transmitted is an ectotherm organism and its life-trait are heavily dependent on weather conditions. Within the project RIS 3 “MOSQUITO VISION”, weather information is ingested as an input to a predictive model for nuisance at evening hours, mainly produced by *Aedes caspius* and, during the night, predominantly provoked by *Culex pipiens*. This information consists of surface observations from several automated weather stations

(AWSs) in the region of Central Macedonia, Greece and a state-of-the-art numerical weather prediction (NWP) modeling system.

In this study, we assess the performance of the NWP system through standard verification methods, and we investigate the impact of two different data assimilation techniques within the first forecast day ($T + 12$ h to $T + 36$ h).

2. Materials and Methods

The non-hydrostatic Weather Research and Forecasting (WRF) modeling system with the Advanced Research (ARW) dynamical core (v.4.1.2) [4,5] was used for the purposes of this study. The model was integrated in two domains (Figure 1a), one covering the Central and East Mediterranean (WRF-D01) and the other encompassing the wider area of Central Macedonia of Greece (WRF-D02, Figure 1a), while their respective horizontal discretization was $10\text{ km} \times 10\text{ km}$ (WRF-D01) and $2\text{ km} \times 2\text{ km}$ (WRF-D02). The analyses and forecast data from the 12 UTC initialization cycles of the Global Forecast System (GFS) were used as initial and boundary conditions (every 3 h) in all numerical experiments.

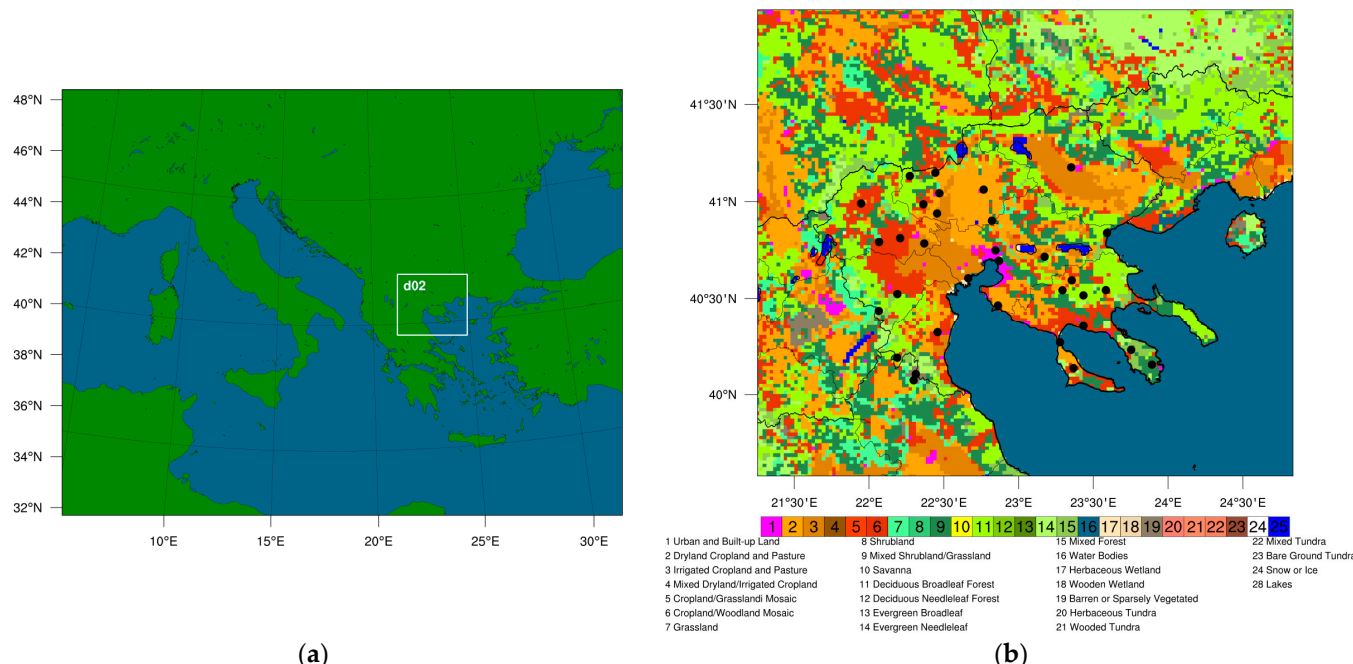


Figure 1. (a) Domain configuration of the WRF-ARW model; (b) land-use categories according to USGS classification system in WRF-D02. Black dots show the location of the automated weather stations of the Region of Central Macedonia climate data hub.

Microphysical processes were parametrized using WSM6 scheme [6], longwave and shortwave radiation were represented by RRTMG scheme [7], boundary layer by YSU scheme [8], surface layer by Monin–Obukhov scheme [9] and soil physics by NOAH-MP model [10,11]. Grell–Freitas ensemble scheme [12] was used for the parametrization of the sub-grid scale convection only on parent domain (WRF-D01). CORINE 2018 [13] data were reclassified into USGS land-use categories [14] and were utilized for the representation of land cover in the model (Figure 1b).

Three different groups of numerical experiments were performed in which each simulation had 36 h as forecast window and was initialized the day before. The simulated period was from 15 July to 1 November 2022 in each experiment. In the control experiment (CNTRL), the model was configured and integrated as presented above with no ingestion of surface observations from the available meteorological stations in the region of interest (RCM, Figure 1b). The second experiment (WRFDA) employed a three-dimensional variational (3DVar) data assimilation technique to create an improved estimate of the

atmospheric state in the region of interest (WRF-D02) by ingesting the available surface observations. For this, the model-space data assimilation system from the MMM Laboratory of NCAR was used. Here, the background error covariance estimation was based on the application of the National Meteorological Center (NMC) method [15,16], in which 184 forecast cycles were utilized. The third experiment (OBSNUDG) facilitated the use of observation nudging data assimilation technique or station nudging. While, in CNTRL and WRFDA experiments, the initialization of WRF-D02 was at 18 UTC, in OBSNUDG experiments the nested domain was initialized at 12 UTC to ingest all the available observations between 12 UTC and 18 UTC.

The in situ surface observations were retrieved from the Region of Central Macedonia (RCM) climate data hub, an initiative that began during the project MOSQUITO VISION (RIS 3, KMP6_077890). Currently, the hub hosts 49 meteorological stations, owned by the Ministry of Environment and Energy, Region of Central Macedonia (RCM), Aristotle University of Thessaloniki (AUTH), ECODEVELOPMENT SA and NOVAGREEN SA.

The model performance in each experiment was assessed in terms of 2 m air temperature (TMP) and relative humidity (RH) and 10 m wind speed (WIND), using the available records from 34 stations of the RCM climate data hub (Figure 1b). The NCEP Unified Post Processing System (UPP) for WRF (v4.1) [17] was used for extracting the simulated meteorological variables under examination, while all the verification metrics were calculated using the Model Evaluation Tools (MET, v8.1.2) [18].

3. Results and Discussion

Table 1 and Figure 2a,c,e present the aggregated verification metrics (Mean Error, ME; Multiplicative Bias, MBIAS; Root Mean Square Error, RMSE; Pearson Correlation Coefficient, PR_COR) in each experiment for each variable under examination. The results indicate that the TMP and WIND were overestimated, and the RH was underestimated by the model in all experiments. These warmer and drier simulated conditions can be linked with the Clausius–Clapeyron equation. However, the direction of the errors in the TMP and RH can also be attributed to other factors like soil moisture, which in turn affects the sensible and latent heat fluxes. Although the simulated WIND values are more than double against observations ($2.37 < \text{MBIAS} < 2.39$), the latter is mostly attributed to the different heights between the observed and simulated wind speeds (most of the observed wind speed values were at approximately 3 m above ground level).

Table 1. Mean Error (ME), Multiplicative (MBIAS), Root Mean Square Error (RMSE) and Pearson Correlation Coefficient (PR_COR) of the simulated 2 m air temperature (TMP) and relative humidity (RH) and 10 m wind speed (WIND) from NODA, WRFDA and OBSNUDG experiments.

Parameter	ME/MBIAS ¹				MAE ¹				RMSE ¹				PR_COR		
	NODA	WRFDA	OBSN	NODA	WRFDA	OBSN	NODA	WRFDA	OBSN	NODA	WRFDA	OBSN			
TMP (K)	0.48 (0.44, 0.52)	0.65 (0.61, 0.70)	0.61 (0.56, 0.65)	1.76 (1.73, 1.79)	1.77 (1.74, 1.80)	1.74 (1.71, 1.77)	2.33 (2.28, 2.37)	2.35 (2.31, 2.39)	2.32 (2.28, 2.37)	0.92	0.92	0.92			
	0.82	0.81	0.80	13.93	14.23	14.45	17.28	17.58	17.54						
RH (%)	(0.81, 0.82)	(0.80, 0.81)	(0.80, 0.81)	(13.73, 14.13)	(14.03, 14.44)	(14.24, 14.65)	(17.05, 17.52)	(17.34, 17.81)	(17.54, 18.02)	0.69	0.69	0.69			
	2.39	2.39	2.37	1.79	1.79	1.78	2.26	2.27	2.26						
WIND (ms ⁻¹)	(2.34, 2.44)	(2.34, 2.44)	(2.32, 2.43)	(1.76, 1.82)	(1.77, 1.82)	(1.75, 1.81)	(2.22, 2.31)	(2.22, 2.31)	(2.21, 2.30)	0.37	0.37	0.38			

¹ Values in parentheses are the bootstrap confidence low and upper limits at 95% significance.

The MAEs range from 1.74 to 1.76 K, 13.93 to 14.45% and 1.78 to 1.79 ms⁻¹ for TMP, RH and WIND, respectively, while the RMSEs are between 2.32 and 2.35 K, 17.28 and 17.58% and 2.26 and 2.27 ms⁻¹. These values are in line with the documented values for Greece and the Mediterranean [19–22]. The OBSNUDG experiment shows the lowest MAE values in TMP (1.74 K) and WIND (1.78 ms⁻¹) against the other two experiments (NODA and WRFDA). The latter is also true for the RMSEs. Finally, the NODA experiment presents the lowest MAE and RMSE regarding RH.

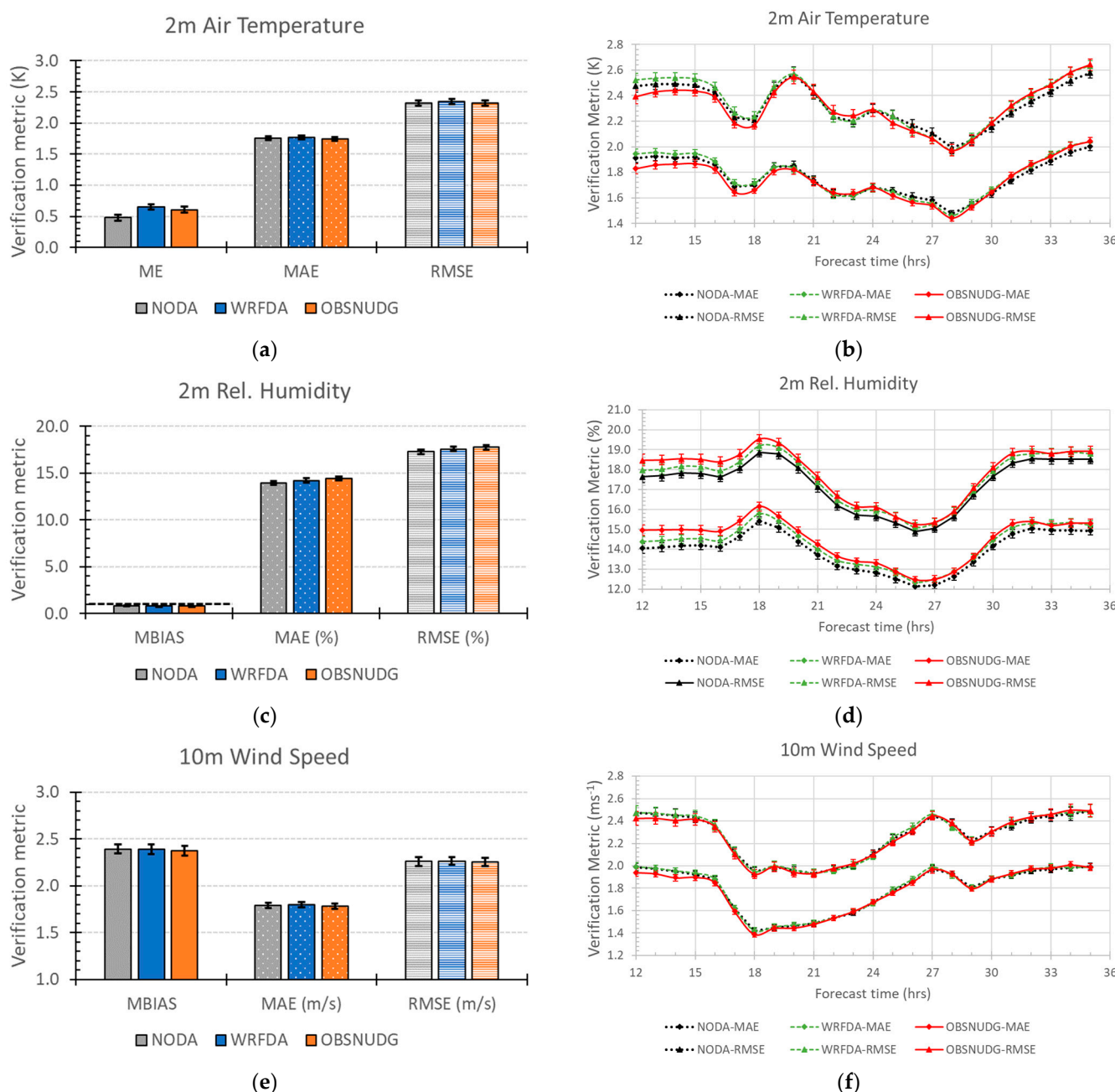


Figure 2. Mean Error/Multiplicative Bias (ME/MBIAS), Mean Absolute Error (MAE) and Root Mean Square Error (RMSE) from NODA (gray bars), WRFDA (blue bars) and OBSNUDG (orange bars) experiments for (a) 2 m air temperature; (c) 2 m relative humidity; and (e) 10 m wind speed, MAE and RSME from NODA (black dotted lines), WRFDA (green dashed lines) and OBSNUDG (red solid lines) experiments as a function of forecast lead time for (b) 2 m air temperature; (d) 2 m relative humidity; and (f) 10 m wind speed.

The temporal evolution of the TMP, RH and WIND errors is displayed in Figure 2b,d,f for each experiment. According to Figure 2b, the ingestion of the available near-surface temperature observations affects the modeled temperatures mostly at the early forecast hours, albeit the differences are quite small among the experiments. Lower TMP errors are presented up to the T + 18 forecast hour when the observational nudging technique (OBSNUGD) is applied. On the other hand, the improved estimate of the atmospheric state in the region of interest through the implementation of the 3Dvar assimilation (WRFDA) shows no improvement in the performance of the model against the NODA experiment. The

latter may be attributed to several factors, including a) the calculation of the background error statistics, a parameter that is of paramount importance in the application of the 3DVar technique, and b) the requirement of additional observations like soundings (TEMP records), satellite (e.g., radiances) or radar (e.g., Doppler velocity and reflectivity) data. In addition, neither of the two assimilation techniques improved the RH errors over time in comparison with the CNTRL experiment. To understand the physical link between TMP and RH errors, additional investigation is required and has been planned. Finally, the simulated WIND was affected positively in OBSNUDG experiment.

This study paves the way for additional investigation on the added value of assimilating observations in an operational forecasting system over the RCM region. Since the analysis was carried out over a relatively long period of time (15 July to 1 November 2022), the results may vary in cases of extreme events (e.g., heatwaves or extreme precipitation) or in certain synoptic weather conditions [23].

Author Contributions: Conceptualization, S.K. and E.K.; methodology, S.K.; software, S.K. and M.-C.K.; validation, S.K.; formal analysis, S.K. and M.-C.K.; investigation, S.K. and E.K.; resources, E.K., S.G. and S.M.; data curation, S.K.; writing—original draft preparation, S.K.; writing—review and editing, S.K., E.K., M.-C.K., S.G. and S.M.; visualization, S.K. and M.-C.K.; supervision, E.K.; project administration, S.M.; funding acquisition, E.K. and S.M. All authors have read and agreed to the published version of the manuscript.

Funding: This study was funded under the Greek Research and Innovation Strategies for Smart Specialization call (RIS 3, project code: KMP6_077890) of the Action «Investment Plans of Innovation» of the Operational Program “Central Macedonia 2014–2020”.

Institutional Review Board Statement: Not applicable.

Informed Consent Statement: Not applicable.

Data Availability Statement: The data presented in this study are available on request from the corresponding author.

Acknowledgments: We would like to acknowledge the AUTH Scientific Computing Centre Infrastructure and technical support. We thank NCEP for providing the GFS operational analyses and forecasts through the NOMADS-ftpprd infrastructure. We acknowledge the use of the WRF-ARW modeling system and the WRF Data Assimilation (WRFDA) System, which were developed at the National Center for Atmospheric Research (NCAR). We thank UCAR/DTC, USGS and CORINE for providing the Model Evaluation Tools (MET) and Unified Post Processing System (UPP) software and the gridded land-use input data. For analysis and visualization purposes, the NCAR Command Language (NCL; v.6.6.2) and Microsoft Office were utilized.

Conflicts of Interest: The authors declare no conflict of interest. The funders had no role in the design of the study; in the collection, analyses or interpretation of data; in the writing of the manuscript; or in the decision to publish the results.

References

1. Papa, A.; Danis, K.; Baka, A.; Bakas, A.; Dougas, G.; Lytras, T.; Theocharopoulos, G.; Chrysagis, D.; Vassiliadou, E.; Kamaria, F.; et al. Ongoing Outbreak of West Nile Virus Infections in Humans in Greece, July–August 2010. *Eurosurveillance* **2010**, *15*, 19644. [[CrossRef](#)]
2. Tsioka, K.; Gewehr, S.; Pappa, S.; Kalaitzopoulou, S.; Stoikou, K.; Mourelatos, S.; Papa, A. West Nile Virus in Culex Mosquitoes in Central Macedonia, Greece, 2022. *Viruses* **2023**, *15*, 224. [[CrossRef](#)]
3. ECDC European Centre for Disease Prevention and Control Weekly Updates: 2022 West Nile Virus Transmission Season. Available online: <https://www.ecdc.europa.eu/en/west-nile-fever/surveillance-and-disease-data/disease-data-ecdc> (accessed on 25 May 2023).
4. Skamarock, W.C.; Klemp, J.B.; Dudhia, J.; Gill, D.O.; Zhiqian, L.; Berner, J.; Wang, W.; Powers, J.G.; Duda, M.G.; Barker, D.M.; et al. *A Description of the Advanced Research WRF Model Version 4.1* (No. NCAR/TN-556+STR); National Center for Atmospheric Research (NCAR): Boulder, CO, USA, 2019; p. 145. [[CrossRef](#)]
5. Wang, W.; Bruyère, C.; Duda, M.G.; Dudhia, J.; Gill, D.O.; Kavulich, M.; Werner, K.; Chen, M.; Lin, H.-C.; Michalakes, J.; et al. *ARW Version 4 Modeling System User’s Guide*; Mesoscale & Microscale Meteorology Division, National Center for Atmospheric Research: Boulder, CO, USA, 2019; p. 408.

6. Hong, S.-Y.; Lim, J.-O.J. The WRF Single-Moment 6-Class Microphysics Scheme (WSM6). *J. Korean Meteorol. Soc.* **2006**, *42*, 129–151.
7. Iacono, M.J.; Delamere, J.S.; Mlawer, E.J.; Shephard, M.W.; Clough, S.A.; Collins, W.D. Radiative Forcing by Long-Lived Greenhouse Gases: Calculations with the AER Radiative Transfer Models. *J. Geophys. Res.* **2008**, *113*, D13103. [[CrossRef](#)]
8. Hong, S.-Y.; Noh, Y.; Dudhia, J. A New Vertical Diffusion Package with an Explicit Treatment of Entrainment Processes. *Mon. Weather. Rev.* **2006**, *134*, 2318–2341. [[CrossRef](#)]
9. Jiménez, P.A.; Dudhia, J.; González-Rouco, J.F.; Navarro, J.; Montávez, J.P.; García-Bustamante, E. A Revised Scheme for the WRF Surface Layer Formulation. *Mon. Weather. Rev.* **2012**, *140*, 898–918. [[CrossRef](#)]
10. Niu, G.-Y.; Yang, Z.-L.; Mitchell, K.E.; Chen, F.; Ek, M.B.; Barlage, M.; Kumar, A.; Manning, K.; Niyogi, D.; Rosero, E.; et al. The Community Noah Land Surface Model with Multiparameterization Options (Noah-MP): 1. Model Description and Evaluation with Local-Scale Measurements. *J. Geophys. Res.* **2011**, *116*, D12109. [[CrossRef](#)]
11. Yang, Z.-L.; Niu, G.-Y.; Mitchell, K.E.; Chen, F.; Ek, M.B.; Barlage, M.; Longuevergne, L.; Manning, K.; Niyogi, D.; Tewari, M.; et al. The Community Noah Land Surface Model with Multiparameterization Options (Noah-MP): 2. Evaluation over Global River Basins. *J. Geophys. Res.* **2011**, *116*, D12110. [[CrossRef](#)]
12. Grell, G.A.; Freitas, S.R. A Scale and Aerosol Aware Stochastic Convective Parameterization for Weather and Air Quality Modeling. *Atmos. Chem. Phys.* **2014**, *14*, 5233–5250. [[CrossRef](#)]
13. EEA Corine Land Cover (CLC) 2018 2019. Available online: https://land.copernicus.eu/pan-european/corine-land-cover/clc2_018 (accessed on 25 May 2023).
14. Pineda, N.; Jorba, O.; Jorge, J.; Baldasano, J.M. Using NOAA AVHRR and SPOT VGT Data to Estimate Surface Parameters: Application to a Mesoscale Meteorological Model. *Int. J. Remote Sens.* **2004**, *25*, 129–143. [[CrossRef](#)]
15. Parrish, D.F.; Derber, J.C. The National Meteorological Center's Spectral Statistical-Interpolation Analysis System. *Mon. Wea. Rev.* **1992**, *120*, 1747–1763. [[CrossRef](#)]
16. Wang, H.; Huang, X.-Y.; Sun, J.; Xu, D.; Zhang, M.; Fan, S.; Zhong, J. Inhomogeneous Background Error Modeling for WRF-Var Using the NMC Method. *J. Appl. Meteorol. Climatol.* **2014**, *53*, 2287–2309. [[CrossRef](#)]
17. DTC NCEP Unified Post Processing System (UPP) for WRF 2020. Available online: <https://dtcenter.org/community-code/unified-post-processor-upp-wrf> (accessed on 25 May 2023).
18. Newman, K.; Jensen, T.; Brown, B.; Fowler, T.; Halley-Gotway, J. *The Model Evaluation Tools v8.1 (METv8.1) User's Guide*; Developmental Testbed Center: Boulder, CO, USA, 2018; p. 437.
19. Papadopoulos, A.; Katsafados, P. Verification of Operational Weather Forecasts from the POSEIDON System across the Eastern Mediterranean. *Nat. Hazards Earth Syst. Sci.* **2009**, *9*, 1299–1306. [[CrossRef](#)]
20. Tegoulia, I.; Pytharoulis, I.; Kotsopoulos, S.; Bampzelis, D.; Kartsios, S.; Karacostas, T. The Influence of WRF Parameterisation Schemes on High Resolution Simulations over Central Greece. In Proceedings of the 15th Annual WRF Users' Workshop, Boulder, CO, USA, 25 June 2014.
21. Pytharoulis, I.; Tegoulia, I.; Kotsopoulos, S.; Bampzelis, D.; Karacostas, T.; Katragkou, E. Verification of the Operational High-Resolution WRF Forecasts Produced by WaveForUs Project. In Proceedings of the 16th Annual WRF Users' Workshop, Boulder, CO, USA, 15–19 June 2015.
22. Kartsios, S.; Karacostas, T.S.; Pytharoulis, I.; Tegoulia, I.; Kotsopoulos, S.; Bampzelis, D. Impact of High Resolution Elevation and Land Use Data on Simulated Convective Activity over Central Greece. In Proceedings of the 95th American Meteorological Society Annual Meeting, Phoenix, AZ, USA, 4–8 January 2015.
23. Karacostas, T.; Kartsios, S.; Pytharoulis, I.; Tegoulia, I.; Bampzelis, D. Observations and Modelling of the Characteristics of Convective Activity Related to a Potential Rain Enhancement Program in Central Greece. *Atmos. Res.* **2018**, *208*, 218–228. [[CrossRef](#)]

Disclaimer/Publisher's Note: The statements, opinions and data contained in all publications are solely those of the individual author(s) and contributor(s) and not of MDPI and/or the editor(s). MDPI and/or the editor(s) disclaim responsibility for any injury to people or property resulting from any ideas, methods, instructions or products referred to in the content.